INTERNATIONAL JOURNAL FOR NUMERICAL METHODS IN FLUIDS
Int. J. Numer. Meth. Fluids 2004; **44**:55–70 (DOI: 10.1002/fld.622)

Calculation of curved open channel flow using physical curvilinear non-orthogonal co-ordinates

Mu-Lan Zhu[1,*,†], Yasuyuki Shimizu[2,‡] and Naoshi Nishimoto[3,§]

[1] *Hydro-soft Technology Institute Co., Ltd. Musashino BLDG. 6F, 3-11-8, Kandanishiki-cho, Chiyoda-ku, Tokyo 101-0054, Japan*
[2] *Civil Engineering Department, Engineering Faculty, Hokkaido University, Kita-Ku, Kita-13, Nishi-8, Sapporo 060-8628, Japan*
[3] *River Engineering Division, NIKKEN Consultants, Inc. Shin-Onarimon Building, 6-17-19, Shinbashi, Minato-Ku, Tokyo 105-0004, Japan*

SUMMARY

There are two main difficulties in numerical simulation calculations using FD/FV method for the flows in real rivers. Firstly, the boundaries are very complex and secondly, the generated grid is usually very non-uniform locally. Some numerical models in this field solve the first difficulty by the use of physical curvilinear orthogonal co-ordinates. However, it is very difficult to generate an orthogonal grid for real rivers and the orthogonal restriction often forces the grid to be over concentrated where high resolution is not required. Recently, more and more models solve the first difficulty by the use of generalized curvilinear co-ordinates (ξ, η). The governing equations are expressed in a covariant or contra-variant form in terms of generalized curvilinear co-ordinates (ξ, η). However, some studies in real rivers indicate that this kind of method has some undesirable mesh sensitivities. Sharp differences in adjacent mesh size may easily lead to a calculation stability problem or even a false simulation result. Both approaches used presently have their own disadvantages in solving the two difficulties that exist in real rivers. In this paper, the authors present a method for two-dimensional shallow water flow calculations to solve both of the main difficulties, by formulating the governing equations in a physical form in terms of physical curvilinear non-orthogonal co-ordinates (s, n). Derivation of the governing equations is explained, and two numerical examples are employed to demonstrate that the presented method is applicable to non-orthogonal and significantly non-uniform grids. Copyright © 2004 John Wiley & Sons, Ltd.

KEY WORDS: generalized curvilinear co-ordinates; physical curvilinear non-orthogonal co-ordinates; generalized-co-ordinate space; physical space; contra-variant; transformation

1. INTRODUCTION

Real rivers usually include compound channels consisting of a low-water channel and a high-water channel. There is not only the external boundary of the high-water channel but also the

*Correspondence to: Mu-Lan Zhu, Hydro-soft Technology Institute Co. Ltd, Musashino Building 6F, 3-11-8 Kandanishiki-cho, Chiyoda-ku, 101-0054 Tokyo, Japan.
†E-mail: zhuml@hydro-soft.com
‡E-mail: yasu@eng.hokudai.ac.jp
§E-mail: nishimoto@nikken.con.co.jp

Received 19 June 2000
Revised 20 May 2003

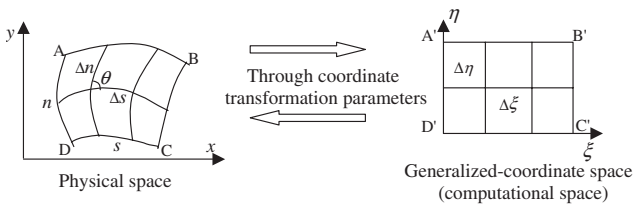

Figure 1. The mapping from physical domain to generalized-co-ordinate domain.

internal boundary of the low-water channel. Two difficulties exist in the numerical simulation for this kind of flowfield. (a) The computational boundaries for this kind of flowfield do not coincide with co-ordinate lines in the Cartesian co-ordinate system (x, y), making the imposition of boundary conditions difficult. (b) It is not easy to generate a grid that varies gradually throughout the whole flowfield. Usually, as shown in Figure 3, a sharp difference of adjacent mesh size can exit near the boundary between the low-water and high-water channel, unless a complex process for grid generation is employed.

Some existing numerical models in computational hydraulics, such as the models of Shimizu [1], Liu [2], solved the first difficulty by the use of physical curvilinear orthogonal co-ordinates (s, n). However, this kind of orthogonal co-ordinates have two serious drawbacks in the applications to real rivers. First, it is very difficult and costly to generate an orthogonal grid for real rivers having external and internal boundaries. Second, the grid that satisfies orthogonality may get over concentrated in some regions where high resolution is not required.

Presently, more models have solved the first difficulty by the use of another kind of co-ordinate system called the generalized curvilinear co-ordinates (ξ, η). The generalized co-ordinate domain is constructed so that a computational boundary in physical space coincides with a co-ordinate line in generalized-co-ordinate space (also called computational space). Figure 1 shows the mapping condition from an irregular physical domain to a square generalized-co-ordinate domain, where the non-uniform curved segments of $\Delta s, \Delta n$ which are non-orthogonal to each other are mapped to the uniform straight segments of $\Delta\xi, \Delta\eta$ which are orthogonal to each other. The mapping not only deforms the boundaries but also transforms the directions and magnitudes of flow variables, that is, it also transforms the governing equations. There are many options in formulating the governing equations transformed from Cartesian co-ordinates (x, y) to generalized curvilinear co-ordinates (ξ, η). The main options can be classified as follows:

(a) The governing equations may be expressed in a semi-contra-variant form in terms of generalized curvilinear co-ordinates (ξ, η), in which the Cartesian velocity of u and the contra-variant velocity of Ucoexist. This is the most extensively used option and most of the numerical models in computational hydraulics are developed in this way. However, this kind of method has two problems. First, the velocity variables should be arranged at the boundary of a control volume in generalized-co-ordinate space (ξ, η) when using a staggered mesh, but it is impossible to arrange the Cartesian velocity in this way. Secondly, the method suffers from a problem of undesirable mesh sensitivities. According to some theoretical error analyses [3], additional errors associated with the use of generalized curvilinear co-ordinates (ξ, η) may be significant and consequently, result in a computational stability problem if non-uniformity

of the grid in physical space is considerable. Therefore, it is necessary when using this method to have the generated grid in the physical domain grow slowly.

(b) The governing equations may be expressed in a complete-contra-variant form in terms of generalized curvilinear co-ordinates (ξ, η), in which the Cartesian velocity is no longer involved. This method eliminates the first problem stated in (a) which is caused by the coexisting of Cartesian velocity, but still retains the disadvantage of undesirable mesh sensitivities like that in (a). Koshizuka *et al.* [4–6] show, theoretically as well as numerically, that stability problems may occur when the mesh size of the adjacent cells differ by more than a factor of 3.

From the above descriptions, it can be seen that both of the two extensively used co-ordinate systems in computational hydraulics have their own disadvantages in the application to real rivers. Physical curvilinear orthogonal co-ordinates (s, n) which is a kind of co-ordinate system in physical space suffers from a problem of orthogonal restriction, although it has little problem on mesh sensitivities. By contrast, generalized curvilinear co-ordinate (ξ, η), which is a kind of co-ordinate system in computational space, suffers from a problem of mesh sensitivities, although orthogonality is no longer restricted. It is the above weaknesses in the existing models that motivate our studies to find a new method applicable to the severe calculation conditions in real rivers, namely, to find a new method applicable to non-orthogonal and significantly non-uniform grid.

Our objective can be achieved through solving the problem of undesirable mesh sensitivities in the use of generalized curvilinear co-ordinates (ξ, η). In order to reduce mesh sensitivities, Demirdzic *et al.* [7], Koshizuka [4–6] and Takizawa *et al.* [8] introduce the use of a physical component that was proposed by Truesdell originally. The governing equations are thus expressed in a contra-variant physical component form in physical space. Their studies indicate that this kind of formulation will improve greatly the tolerance to the grid's non-uniformity.

Based on their methodology, the authors derive the transformed governing equations for two-dimensional shallow water flows, expressed in a physical form in physical space. The transformed governing equations completely eliminate the abstract and obtuse notions related to co-ordinate transformation parameters, and are expressed in terms of physical curvilinear non-orthogonal co-ordinates (s, n) which is an extension of the extensively used orthogonal ones. This kind of extension is meaningful for numerical calculations in river engineering. Correctness of the transformed governing equations is verified, and effectiveness of the proposed method to significantly non-uniform grid is demonstrated, with two numerical examples.

Finally, let us sum up and explain the co-ordinate systems mentioned in the paper in order to prevent confusion. (x, y) is the well-known Cartesian co-ordinate system. (ξ, η) is the generalized curvilinear co-ordinate system in generalized-co-ordinate space (called computational space also). (s, n) is physical curvilinear co-ordinate system in physical space having two options for the physical curvilinear orthogonal co-ordinate system and physical curvilinear non-orthogonal co-ordinate system.

2. GOVERNING EQUATIONS

In order to abbreviate the expressions of governing equations, we denote co-ordinate system (x, y) as (x^1, x^2), and (ξ, η) as (ξ^1, ξ^2) in Sections 2.1 and 2.2.

2.1. Governing equations in the Cartesian co-ordinate system

Equations (1)–(2) show the two-dimensional shallow water equations in the Cartesian co-ordinate system (x^1, x^2) where viscous effects are neglected for simplicity:

- Momentum equation

$$u^j \frac{\partial u^i}{\partial x^j} = -\frac{1}{\rho}\delta^{ij}\frac{\partial P}{\partial x^j} - \frac{\tau_{x^i}}{\rho h_s} \quad \begin{Bmatrix} i=1,\ j=1,2 \\ i=2,\ j=1,2 \end{Bmatrix} \tag{1}$$

- Continuity equation

$$\frac{\partial (u^i h_s)}{\partial x^i} = 0 \quad (i=1,2) \tag{2}$$

where u^i is the velocity in the x^i direction, P is the pressure $= \rho GH$, and ρ, H, G is the water density, water level and gravitational acceleration $= 9.8\ \mathrm{m}^2/\mathrm{s}$, respectively; h_s is the water depth, δ^{ij} is the Kronecker's delta defined as $\delta^{ij} = 1$ if $i = j$ and $\delta^{ij} = 0$ if $i \neq j$, τ_{x^i} is the a friction stress acting on channel bed in x^i direction and defined as $\tau_{x^i} = (GN^2/\sqrt[3]{R})Vu^i$ in which N is Manning roughness coefficient, R is the hydraulic radius and V is the combined velocity.

2.2. Transformed governing equations expressed in generalized-co-ordinate space

In order to deal with the complicated boundary, the governing equations in the Cartesian co-ordinate system (x^1, x^2) stated in Section 2.1 are mapped into the generalized co-ordinate system (ξ^1, ξ^2). Based on Riemann Geometry, Equations (1)–(2) can be transformed to Equations (3)–(4) expressed in a complete-contra-variant form in terms of generalized curvilinear co-ordinates (ξ^1, ξ^2).

$$U^j \nabla_j U^i = -\frac{1}{\rho} g^{ij} \nabla_j P - \frac{T^i}{\rho h_s} \quad \begin{cases} i=1,\ j=1,2 \\ i=2,\ j=1,2 \end{cases} \tag{3}$$

$$\nabla_i (U^i h_s) = 0 \quad (i=1,2) \tag{4}$$

where U^i, ∇_i, g^{ij} denote contra-variant velocity, covariant differentiation and fundamental contra-variant tensor along ξ^i direction in generalized-co-ordinate space. T^i denotes the contra-variant friction stress along the ξ^i direction and is defined as $T^i = (GN^2/\sqrt[3]{R})VU^i$.

Furthermore, Demirdzic [7] and Koshizuka [4–6] indicate that the introduction of a physical component may greatly improve the tolerance to the grid's non-uniformity during calculation. According to their methodology, Equations (3)–(4) can be further transformed to

$$U^{(j)} \nabla_{(j)} U^{(i)} = -\frac{1}{\rho} g^{(ij)} \nabla_{(j)} P - \frac{T^{(i)}}{\rho h_s} \quad \begin{cases} i=1,\ j=1,2 \\ i=2,\ j=1,2 \end{cases} \tag{5}$$

$$\nabla_{(i)} (U^{(i)} h_s) = 0 \qquad (i=1,2) \tag{6}$$

where $U^{(i)}, \nabla_{(i)}, g^{(ij)}, T^{(i)}$ denote the physical components of $U^i, \nabla_i, g^{ij}, T^i$, respectively. The parentheses of herein are used to denote physical components.

Although the expression of Equations (5)–(6) seems rather simple, it is actually quite complicated when it is unfolded. The momentum equation in the ξ^1 direction unfolded from Equation (5) has an expression as [4–6]:

$$\begin{aligned}
&\frac{1}{\sqrt{g_{11}}}\left[U^{(1)}\frac{\partial U^{(1)}}{\partial \xi^1} - \frac{g_{12}}{g_{11}}\begin{Bmatrix} 2 \\ 1\,1 \end{Bmatrix} U^{(1)}U^{(1)} + \sqrt{\frac{g_{11}}{g_{22}}}\begin{Bmatrix} 1 \\ 2\,1 \end{Bmatrix} U^{(1)}U^{(2)}\right] \\
&\quad + \frac{1}{\sqrt{g_{22}}}\left[U^{(2)}\frac{\partial U^{(1)}}{\partial \xi^2} - \frac{g_{12}}{g_{11}}\begin{Bmatrix} 2 \\ 1\,2 \end{Bmatrix} U^{(1)}U^{(2)} + \sqrt{\frac{g_{11}}{g_{22}}}\begin{Bmatrix} 1 \\ 2\,2 \end{Bmatrix} U^{(2)}U^{(2)}\right] \\
&\quad = -\frac{\sqrt{g_{11}}}{\rho}\left[g^{11}\frac{\partial P}{\partial \xi^1} + g^{12}\frac{\partial P}{\partial \xi^2}\right] - \frac{T^{(1)}}{\rho h_s}
\end{aligned} \tag{7}$$

Equation (7) involves many abstract notations such as fundamental contra- and co-variant tensors g^{ij}, g_{ij}, physical component of contra-variant velocity $U^{(i)}$, and Christoffel symbol $\{{}^{i}_{j\,k}\}$. They make the expression of the equation complicated, and hardly understandable. Moreover, the more complicated the expression, the higher the calculation cost, and the more numerical error it may cause due to discretization. The authors therefore make efforts to further transform Equations (5)–(6), and obtain the governing equations expressed by physical variables in physical space which exclude the mapping parameters between co-ordinate systems and become concise and comparatively understandable.

2.3. *Transformed governing equations expressed in physical space*

The detailed process to transform Equations (5)–(6) to the equations expressed in physical space with physical variables in terms of physical curvilinear non-orthogonal co-ordinates (s, n) can be referred to Appendix A at the end of the paper. The final transformed form of the two-dimensional shallow water governing equations having viscous effects ignored are shown as follows:

- momentum equation in s direction

$$\begin{aligned}
&u_s\frac{\partial u_s}{\partial s} + u_n\frac{\partial u_s}{\partial n} + \frac{\cos\theta}{\sin\theta}\frac{u_s^2}{r_s} - \frac{1}{\sin\theta}\frac{u_n^2}{r_n} + \frac{1}{\sin\theta}\frac{u_s u_n}{[1+(1/k_n)^2]}\frac{\partial(1/k_n)}{\partial s} \\
&\quad - \frac{\cos\theta}{\sin\theta}\frac{u_s u_n}{1+k_s^2}\frac{\partial k_s}{\partial n} + \frac{1}{\sin^2\theta}\frac{1}{\rho}\frac{\partial P}{\partial s} - \frac{\cos\theta}{\sin^2\theta}\frac{1}{\rho}\frac{\partial P}{\partial n} + \frac{\tau_s}{\rho h_s} = 0
\end{aligned} \tag{8}$$

- momentum equation in n direction

$$\begin{aligned}
&u_s\frac{\partial u_n}{\partial s} + u_n\frac{\partial u_n}{\partial n} + \frac{\cos\theta}{\sin\theta}\frac{u_n^2}{r_n} - \frac{1}{\sin\theta}\frac{u_s^2}{r_s} - \frac{\cos\theta}{\sin\theta}\frac{u_s u_n}{[1+(1/k_n)^2]}\frac{\partial(1/k_n)}{\partial s} \\
&\quad + \frac{1}{\sin\theta}\frac{u_s u_n}{1+k_s^2}\frac{\partial k_s}{\partial n} + \frac{1}{\sin^2\theta}\frac{1}{\rho}\frac{\partial P}{\partial n} - \frac{\cos\theta}{\sin^2\theta}\frac{1}{\rho}\frac{\partial P}{\partial s} + \frac{\tau_n}{\rho h_s} = 0
\end{aligned} \tag{9}$$

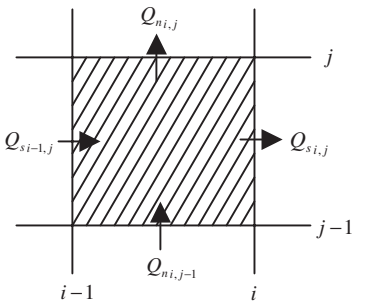

Figure 2. The discharges into and out from control volume.

- continuity equation

$$\frac{\partial(Au_s h_s)}{\partial s} + \frac{\partial(Au_n h_s)}{\partial n} = 0 \tag{10}$$

where u_s, u_n denote the velocities in s, n direction in physical space, respectively, θ denotes the angle between s and n lines, r_s, r_n denote the curvature radii of s and n line, respectively, and k_s, k_n denote the inclinations of s and n line, respectively. P denotes pressure, and τ_s, τ_n denote the friction stresses acting on channel bed in s and n direction defined as $\tau_s = (GN^2/\sqrt[3]{R})Vu_s$ and $\tau_n = (GN^2/\sqrt[3]{R})Vu_n$, respectively. The third and fourth term in Equation (8) denote the components of centrifugal forces in s direction caused by the curvatures of s and n line, respectively, and the fifth and sixth term in Equation (8) denote the components of the Corioli forces in s direction caused by the variations of s and n line's inclination, respectively. And similar explanations can be given to the third and fourth term as well as to the fifth and sixth term in Equation (9). A is the area of calculation mesh and defined as $A = \mathrm{d}s \times \mathrm{d}n \times \sin\theta$. In the computation, Equation (10) can be reduced to Equation (11), where $Q_{si-1,j}, Q_{si,j}$ are the discharges into and out of the control volume in the s direction, and $Q_{ni,j-1}, Q_{ni,j}$ are the discharges into and out of the control volume in the n direction as shown in Figure 2

$$Q_{si-1,j} - Q_{si,j} + Q_{ni,j-1} - Q_{ni,j} = 0 \tag{11}$$

In the case of s line orthogonal to n line, there are the relations of $\sin\theta = 1, \cos\theta = 0$, $k_s = -1/k_n$, therefore Equations (8)–(10) can be simplified to the following equations which are completely consistent with the well-known equations in orthogonal curvilinear co-ordinate system [1, 2]:

$$u_s \frac{\partial u_s}{\partial s} + u_n \frac{\partial u_s}{\partial n} - \frac{u_n^2}{r_n} + \frac{u_s u_n}{r_s} + \frac{1}{\rho}\frac{\partial P}{\partial s} + \frac{\tau_s}{\rho h_s} = 0 \tag{12}$$

$$u_s \frac{\partial u_n}{\partial s} + u_n \frac{\partial u_n}{\partial n} - \frac{u_s^2}{r_s} + \frac{u_s u_n}{r_n} + \frac{1}{\rho}\frac{\partial P}{\partial n} + \frac{\tau_n}{\rho h_s} = 0 \tag{13}$$

$$\frac{\partial(Au_s h_s)}{\partial s} + \frac{\partial(Au_n h_s)}{\partial n} = 0 \tag{14}$$

Presently, we ignore the burdensome diffusion term in the governing equation of Equations (8)–(10) for simplification since this is our first step study, and we will address the problem

of the diffusion term which is much more complicated in our next-step study for promoting the practical value of the model.

3. NUMERICAL EXAMPLES

The SIMPLER algorithm, which is a revised SIMPLE algorithm having a more rapid convergence speed, proposed by Pantanker [9] is applied to two numerical examples.

The first example is for verifying the correctness of the newly transformed governing equations. For this purpose, two kinds of grids, which are orthogonal and non-orthogonal, are employed to compute the same example and the consistency of two results is checked. The governing equations of Equations (12)–(14) which are expressed in terms of physical curvilinear orthogonal co-ordinates, are adopted to deal with the case of the orthogonal grid; while the newly inferred governing equations of Equations (8)–(10) are adopted to deal with the case of the non-orthogonal grid.

The second example is for demonstrating that the proposed method can be applied to the extremely non-uniform grid, which often easily leads to a false solution or a problem of computational stability if the governing equations are expressed in a conventional co- or contra-variant form in terms of generalized co-ordinate co-ordinates (ξ, η).

3.1. Example-1

The calculation objective is a meandering channel whose shape is a sine-generated curve expressed as

$$\theta = \theta_{\max} \sin(2\pi s/L) \tag{15}$$

where θ is the angle between the curved centreline and the down-valley axis at an arch distance of s, $\theta_{\max}$ is the maximum value of θ, L is the wavelength measured along the curved centreline. Simulation conditions are shown in Table I. The initial and boundary conditions are adopted as follows:

- *Initial condition*: The initial values of velocity u_s, water depth h_s and water level H are defined by the uniform flow calculation. And the initial value of velocity u_n is defined as 0.
- *Boundary condition*: At upstream $(i = 1)$ and downstream $(i = \text{nend})$: the cyclical conditions of $\phi(1, j) = \phi(\text{nend}, j), \phi(\text{nend} + 1, j) = \phi(2, j)$ are employed.
- *At side wall*: free-slip condition is employed.

The contours of calculated velocities are shown in Plates 1 and 2 where Plate 1 shows the result for orthogonal grid (case 1) and Plate 2 shows the result for non-orthogonal grid

Table I. Simulation condition of Example-1.

Total width of channel (cm)	Length of channel (cm)	$\theta_{\max}$	Discharge $Q(l/s)$	Slope i_b	Manning roughness coefficient
20	220	35°	2.15	0.009	0.015

Table II. A quantitative comparison between the two results of orthogonal and non-orthogonal grid.

	Absolute value	Relative value (%)
Mean difference of the velocity at each grid point	0.0045	1.2
Difference of maximum velocity	0.0043	0.93
Difference of minimum velocity	0.0069	2.1
Difference of mean velocity	0.0054	1.4

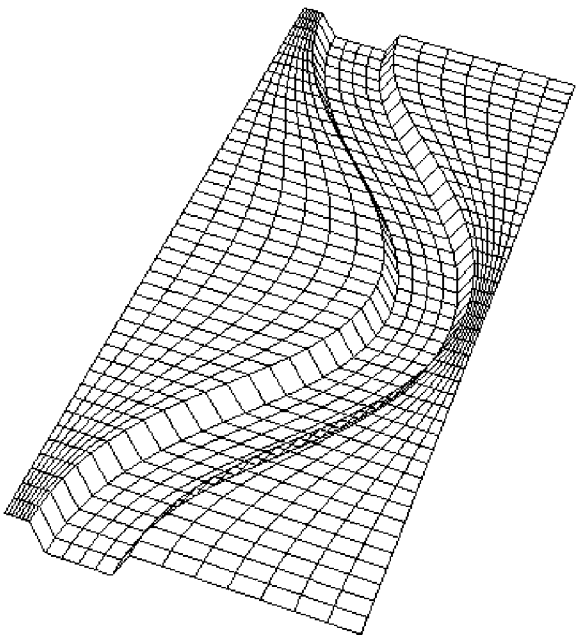

Figure 3. Shape of the artificial river calculated.

(case 2). A quantitative comparison between the two results for the velocity is shown in Table II, where the mean difference and the mean relative difference of velocity at each grid point are evaluated by $\sum_i \sum_j (u_{i,j}^{\text{case1}} - u_{i,j}^{\text{case2}})/(ni \times nj)$ and $\sum_i \sum_j [(u_{i,j}^{\text{case1}} - u_{i,j}^{\text{case2}})/u_{i,j}^{\text{case1}}]/(ni \times nj)$, respectively, in which ni and nj are the total numbers of i and j index, respectively. However, as shown in Plates 1 and 2 the position of each grid point for the two cases is different, we thus take a interpolation to obtain the value of $u_{i,j}^{\text{case2}}$ having the same position as $u_{i,j}^{\text{case1}}$.

From Table II and comparing Plate 1 with Plate 2, it can be seen that the difference between the two results is very small. This performance demonstrates that the proposed method is applicable when the grid is non-orthogonal.

3.2. Example-2

The simulation objective is an artificial river consisting of low-water and high-water channels as shown in Figure 3, where high-water channel is wide at some places and very narrow at

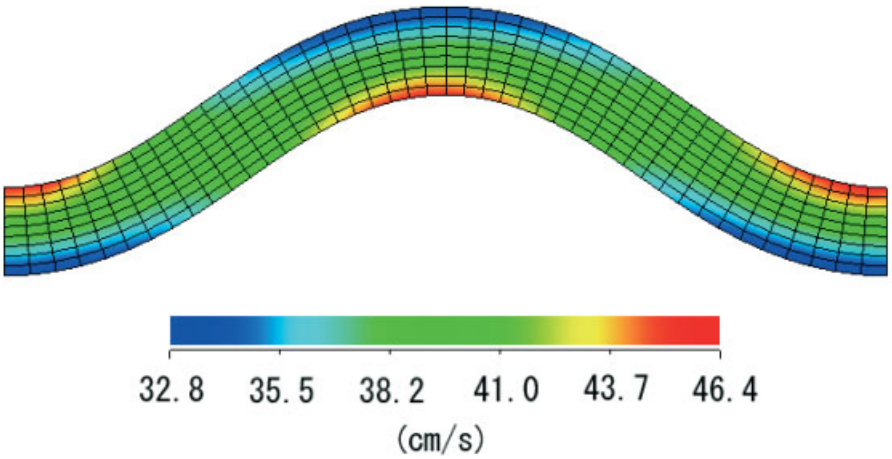

Plate 1. Contour of calculated velocities for orthogonal grid.

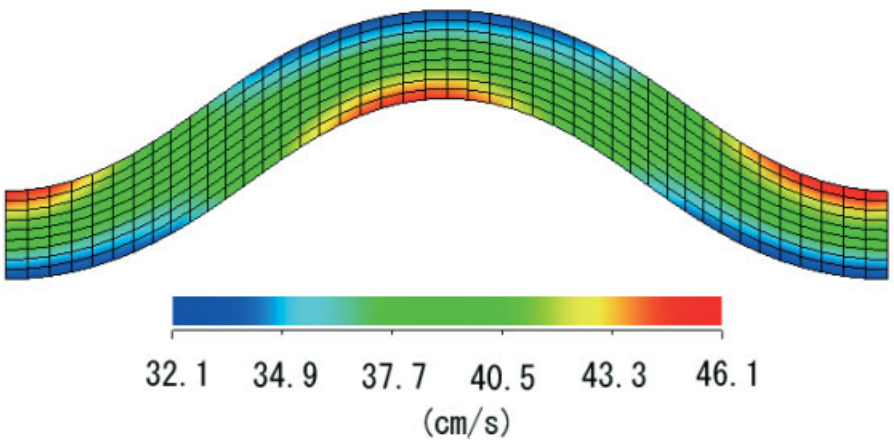

Plate 2. Contour of calculated velocities for non-orthogonal grid.

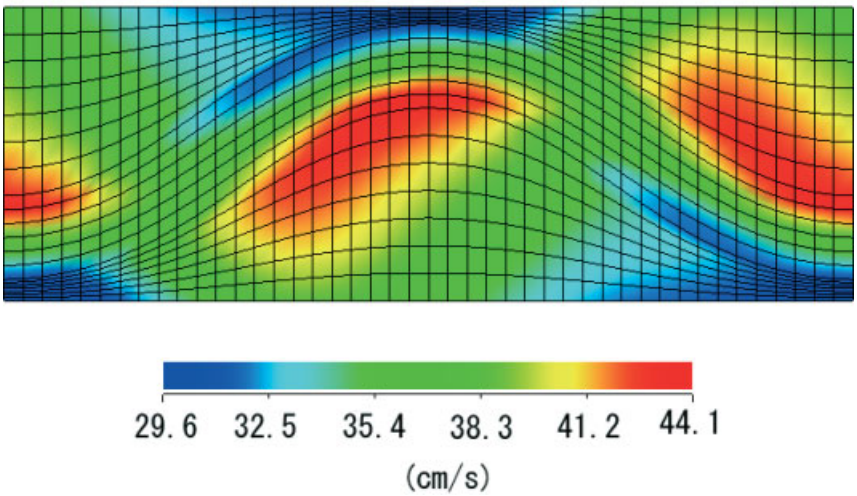

Plate 3. Contour of calculated velocities.

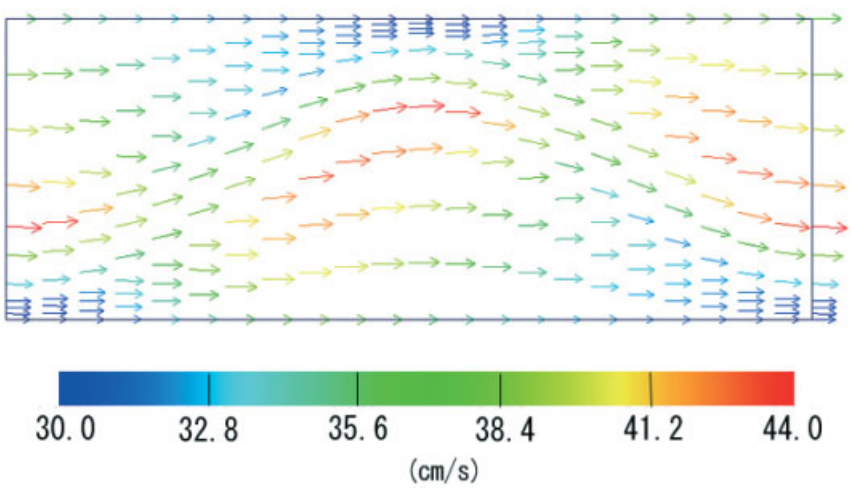

Plate 4. Calculated velocity vectors.

Table III. Simulation condition of Example-2.

Total width of channel (cm)	Width of low-water channel (cm)	Length of channel (cm)	θ_{max}	Discharge $Q(l/s)$	Slope i_b	Manning roughness coefficient
100	20	220	35^0	7.15	0.009	0.015

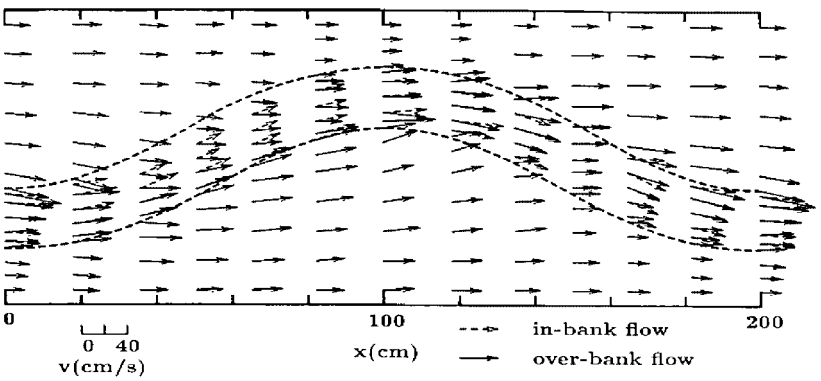

Figure 4. Measured velocity vectors.

other places as in a real river. The low-water channel is the sine-generated curve used in Example-1. It can be seen from Figure 3 that the generated grid is non-orthogonal and the width of grid Δn changes sharply at some place around the boundary between low-water and high-water channel. The simulation conditions are shown in Table III. Initial and boundary conditions are adopted as that of Example-1. Contours of calculated velocity are shown in Plate 3. Vectors of calculated and measured velocities are shown in Plate 4 and Figure 4, respectively. Although the model used is a simple depth-average two-dimensional one, with no special consideration on the mutual effects between low-water and high-water channel, the calculated depth-average velocities basically agree with the measured ones.

It should be stressed that the calculation achieved convergence very easily and quickly, although the width of Δn for the generated grid varies sharply, and the largest variation rate of grid's width $\Delta n_{i,j}/\Delta n_{i,j+1}$ is near to 6. The proposed method is therefore demonstrated to be applicable to the significantly non-uniform grid.

4. CONCLUSION

We have presented a new method that allows calculations to be effective even under the condition that the generated mesh is non-orthogonal and extremely non-uniform locally. The proposed method was demonstrated to be applicable through two numerical examples.

Compared with the use of Equations (5)–(6) expressed in contra-variant physical component form whose unfolded expressions are rather complicated, the governing equations

proposed by the authors are not only more understandable, but also have a more concise expression, since the mapping parameters from physical space to generalized-co-ordinate space are excluded from the equations completely. This leads to simple finite-difference equations and, consequently, to computational economy.

Our next work is to take account of the diffusion terms that were ignored in this study for simplicity.

APPENDIX A

This appendix is contributed to describe how to transform the existing governing equations expressed in a contra-variant physical component form to the proposed governing equations expressed in a physical form. The detailed transformation process will only focus on the momentum equation in ξ direction. As concerns the transformation for the momentum equation in η direction, it is similar to the case in ξ direction and thus omitted here. Also, the transformation of continuity equation is omitted for its simplicity. Again, we point out that the governing equations referred here are the two-dimensional shallow water governing equations having diffusion term ignored.

Equation (A1) shows the momentum equation in ξ direction expressed in a contra-variant physical component form

$$\begin{aligned}
&\frac{1}{\sqrt{g_{11}}}\left[U^{(1)}\frac{\partial U^{(1)}}{\partial \xi^1}-\frac{g_{12}}{g_{11}}\left\{\begin{matrix}2\\1\,1\end{matrix}\right\}U^{(1)}U^{(1)}+\sqrt{\frac{g_{11}}{g_{22}}}\left\{\begin{matrix}1\\2\,1\end{matrix}\right\}U^{(1)}U^{(2)}\right]\\
&\quad+\frac{1}{\sqrt{g_{22}}}\left[U^{(2)}\frac{\partial U^{(1)})}{\partial \xi^2}-\frac{g_{12}}{g_{11}}\left\{\begin{matrix}2\\1\,2\end{matrix}\right\}U^{(1)}U^{(2)}+\sqrt{\frac{g_{11}}{g_{22}}}\left\{\begin{matrix}1\\2\,2\end{matrix}\right\}U^{(2)}U^{(2)}\right]\\
&\quad=-\frac{\sqrt{g_{11}}}{\rho}\left[g^{11}\frac{\partial P}{\partial \xi^1}+g^{12}\frac{\partial P}{\partial \xi^2}\right]-\frac{T^{(1)}}{\rho h_s}
\end{aligned}\tag{A1}$$

where $U^{(i)}$, $T^{(i)}$ denote the physical component of contra-variant velocity U^i and the physical component of contra-variant friction stress T^i. g_{ij}, g^{ij} denote fundamental co-variant tensor and fundamental contra-variant tensor, respectively, and $\{\begin{matrix}i\\j\,k\end{matrix}\}$ denotes Christoffel symbol. The definitions and geometrical meanings of $U^{(i)}$, g_{ij}, g^{ij}, $\{\begin{matrix}i\\j\,k\end{matrix}\}$ described by Demirdzic *et al.* [7] and Koshizuka *et al.* [4–6] are given in the following subsection. It should be pointed out that subscript $_{ij}$ is used to denote co-variant and superscript ^{ij} is used to denote contra-variant throughout the paper.

A.1. Definitions and geometrical meanings

(1a) *Contra-variant physical velocity* $U^{(i)}$:

$$U^{(1)}=\sqrt{g_{11}}U^1=\sqrt{g_{11}}(\xi_x u_x+\xi_y u_y) \tag{A2}$$

$$U^{(2)}=\sqrt{g_{22}}U^2=\sqrt{g_{22}}(\eta_x u_x+\eta_y u_y) \tag{A3}$$

(1b) *Fundamental co- and contra-variant tensors* g_{ij}, g^{ij}:

Fundamental co-variant tensors g_{ij} are also called metric tensor. From the aspect of co-ordinate transformation relation, they have the following relations with the parameters of co-ordinate transformation $x_\xi, x_\eta, y_\xi, y_\eta$:

$$g_{11} = x_\xi^2 + y_\xi^2, \quad g_{12} = g_{21} = x_\xi x_\eta + y_\xi y_\eta, \quad g_{22} = x_\eta^2 + y_\eta^2 \tag{A4}$$

While from the aspect of geometry, g_{ij} can be interpreted as the scale factors which associate the small change $\Delta\xi, \Delta\eta$ in generalized-co-ordinate space with the small changes $\Delta s, \Delta n$ in physical space in the way:

$$\Delta s = \sqrt{g_{11}}\,\Delta\xi, \quad \Delta n = \sqrt{g_{22}}\,\Delta\eta \tag{A5}$$

Also, g_{12} and g_{11}, g_{22} have the relation as

$$g_{12} = g_{21} = \sqrt{g_{11} g_{12}}\cos\theta \tag{A6}$$

where θ denotes the angle between s and n lines as shown in Figure 1. g_{ij} can be also related to well-known Jacobian J by

$$J = (x_\xi y_\eta - x_\eta y_\xi) = \sqrt{|g_{ij}|} = \sqrt{(g_{11}g_{22} - g_{12}g_{21})} = \sqrt{g_{11}g_{22}}\sin\theta \tag{A7}$$

Equation (A7) gives a physical interpretation of Jacobian. Concretely, Jacobian denotes the area in physical space corresponding to the unit area of computational grid in generalized-co-ordinate space.

Besides, contra-variant g^{ij} and co-variant g_{ij} has the following relationship:

$$g_{ij} g^{jk} = \delta^{ik}$$

$$\text{namely,} \begin{bmatrix} g_{11} & g_{12} \\ g_{21} & g_{22} \end{bmatrix} \begin{bmatrix} g^{11} & g^{12} \\ g^{21} & g^{22} \end{bmatrix} = \begin{bmatrix} 1 & 0 \\ 0 & 1 \end{bmatrix} \tag{A8}$$

Thus, the following relations between fundamental co- and contra-variant tensors can be derived out easily based on Equations (A7) and (A8):

$$g^{11} = \frac{g_{22}}{J^2}, \quad g^{12} = -\frac{g_{12}}{J^2}, \quad g^{21} = -\frac{g_{21}}{J^2}, \quad g^{22} = \frac{g_{11}}{J^2} \tag{A9}$$

(1c) *Christoffel symbol* $\left\{ {i \atop j\,k} \right\}$:

The Christoffel symbol $\left\{ {i \atop j\,k} \right\}$ describes that how many variations for the component in i direction are caused when the unit vector in j direction moves unit length along k direction. Specifically, $\left\{ {1 \atop 2\,2} \right\}, \left\{ {2 \atop 1\,1} \right\}$ denote the curvature of computational grid which causes centrifugal force, while $\left\{ {1 \atop 1\,2} \right\}, \left\{ {2 \atop 1\,2} \right\}$ denote the distortion of computational grid which causes Corioli force.

The Christoffel symbol can be defined by the various parameters of co-ordinate transformation as follows:

$$\begin{Bmatrix} 1 \\ 1\,2 \end{Bmatrix} = \frac{1}{J}(y_\eta x_{\xi\eta} - x_\eta y_{\xi\eta}) \quad \begin{Bmatrix} 1 \\ 2\,2 \end{Bmatrix} = \frac{1}{J}(y_\eta x_{\eta\eta} - x_\eta y_{\eta\eta})$$
$$\begin{Bmatrix} 2 \\ 1\,2 \end{Bmatrix} = \frac{1}{J}(x_\xi y_{\xi\eta} - y_\xi x_{\xi\eta}) \quad \begin{Bmatrix} 2 \\ 1\,1 \end{Bmatrix} = \frac{1}{J}(x_\xi y_{\xi\xi} - y_\xi x_{\xi\xi}) \tag{A10}$$

A.2. Transformation of governing equation

Based on the above definitions and geometrical meanings, each term in Equation (A1) can be transformed into physical space as follows:

(1) *Advective term* 1 $(1/\sqrt{g_{11}})U^{(1)}\partial U^{(1)}/\partial\xi$:

There are some relations between parameters of co-ordinate transformation as

$$\xi_x = \frac{y_\eta}{J}, \xi_y = -\frac{x_\eta}{J}, \eta_x = -\frac{y_\xi}{J}, \eta_y = \frac{x_\xi}{J} \tag{A11}$$

thus, we may have

$$\begin{aligned} U^{(1)} &= \sqrt{g_{11}}U^1 = \sqrt{g_{11}}(\xi_x u_x + \xi_y u_y) = \sqrt{g_{11}}\left(\frac{y_\eta}{J}u_x - \frac{x_\eta}{J}u_y\right) \\ &= \sqrt{g_{11}}\left(\frac{y_\eta}{\sqrt{g_{11}g_{22}}\sin\theta}u_x - \frac{x_\eta}{\sqrt{g_{11}g_{22}}\sin\theta}u_y\right) = \frac{1}{\sin\theta}\left(\frac{\partial y}{\partial n}u_x - \frac{\partial x}{\partial n}u_y\right) \end{aligned} \tag{A12}$$

where θ denotes the angle between s and n line.

Let α denote the angle between s line and x co-ordinate, β denote the angle between n line and x co-ordinate and u_s, u_n denote velocities along s, n lines in physical space, respectively. One may easily get the following relations:

$$\frac{\partial y}{\partial n} = \sin\beta, \quad \frac{\partial x}{\partial n} = \cos\beta \tag{A13}$$

$$u_x = u_s\cos\alpha + u_n\cos\beta, \quad u_y = u_s\sin\alpha + u_n\sin\beta \tag{A14}$$

Putting Equations (A13)–(A14) into Equation (A12), we get

$$\begin{aligned} U^{(1)} &= \frac{1}{\sin\theta}[\sin\beta(u_s\cos\alpha + u_n\cos\beta) - \cos\beta(u_s\sin\alpha + u_n\sin\beta] \\ &= \frac{1}{\sin\theta}u_s(\sin\beta\cos\alpha - \cos\beta\sin\alpha) = u_s\frac{\sin(\beta-\alpha)}{\sin\theta} = u_s\frac{\sin\theta}{\sin\theta} = u_s \end{aligned} \tag{A15}$$

Equation (A15) indicates that the contra-variant physical velocity component $U^{(1)}$ actually is the physical velocity u_s along s line in physical space.

Therefore, we may have

$$\frac{1}{\sqrt{g_{11}}}U^{(1)}\frac{\partial U^{(1)}}{\partial \xi}=U^{(1)}\frac{\partial U^{(1)}}{\sqrt{g_{11}}\partial \xi}=u_s\frac{\partial u_s}{\partial s} \tag{A16}$$

(2) *Advective term* 2:

Similar to $U^{(1)}$, it can also be deduced that $U^{(2)}$ actually is the physical velocity u_n along n line in physical space.

$$\frac{1}{\sqrt{g_{22}}}U^{(2)}\frac{\partial U^{(1)}}{\partial \eta}=U^{(2)}\frac{\partial U^{(1)}}{\sqrt{g_{22}}\partial \eta}=u_n\frac{\partial u_s}{\partial n} \tag{A17}$$

(3) *Source term* (1a) (*centrifugal force caused by the curvature of s line*):

$$\begin{aligned}
-\frac{1}{\sqrt{g_{11}}}\frac{g_{12}}{g_{11}}\left\{\begin{matrix}2\\1\ 1\end{matrix}\right\}U^{(1)}U^{(1)}&=-\frac{\sqrt{g_{11}g_{22}}\cos\theta}{\sqrt{g_{11}}g_{11}}\frac{1}{J}(x_\xi y_{\xi\xi}-y_\xi x_{\xi\xi})u_s^2\\
&=-\frac{\cos\theta}{\sin\theta}\frac{1}{g_{11}^{3/2}}x_\xi^2\frac{\partial}{\partial\xi}\left(\frac{y_\xi}{x_\xi}\right)u_s^2=-\frac{\cos\theta}{\sin\theta}\frac{x_\xi^2}{(x_\xi^2+y_\xi^2)^{3/2}}\left[\frac{\partial}{\partial x}\left(\frac{y_\xi}{x_\xi}\right)x_\xi\right]u_s^2\\
&=-\frac{\cos\theta}{\sin\theta}\frac{1}{[(1+y_\xi^2/x_\xi^2)]^{3/2}}\frac{\partial}{\partial x}\left(\frac{\partial y}{\partial x}\right)u_s^2=-\frac{\cos\theta}{\sin\theta}\frac{y_{xx}}{[1+(y_x)^2]^{3/2}}u_s^2\\
&=+\frac{\cos\theta}{\sin\theta}\frac{u_s^2}{r_s}
\end{aligned} \tag{A18}$$

where r_s is the curvature radius of s line. An attention should be paid for the sign definition of r_s. It can be seen from Equation (A18) that source term (1a) will be equal to 0 if s line is orthogonal to n line. However, when s line is not orthogonal to n line, the centrifugal force u_s^2/r_s caused by the curvature of s line acting on the direction orthogonal to s line, can be divided into two components of force along the directions of s and n lines as shown in Figure A1. Based on the elementary geometry, it is easy to obtain its two force components along s and n line to be $-\cot\theta\, u_s^2/r_s$ and $+(1/\sin\theta)u_s^2/r_s$, respectively, and be $\cot\theta\, u_s^2/r_s$ and $-(1/\sin\theta)u_s^2/r_s$ when they are moved to the left side of equation. This result coincides with Equation (A18) completely.

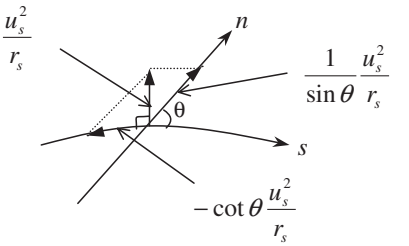

Figure A1. Two force components of u_s^2/r_s along s and n directions.

(4) *Source term* (1b) (*centrifugal force caused by the curvature of n line*):
Similar to (3), we may have

$$\frac{1}{\sqrt{g_{22}}}\sqrt{\frac{g_{11}}{g_{22}}}\begin{Bmatrix}1\\2\,2\end{Bmatrix}U^{(2)}U^{(2)}=\sqrt{\frac{g_{11}}{g_{22}}}\frac{1}{J}(y_\eta x_{\eta\eta}-x_\eta y_{\eta\eta})u_n^2=-\frac{1}{\sin\theta}\frac{u_n^2}{r_n} \tag{A19}$$

(5) *Source term* (2a) (*Corioli force caused by the s line's distortion of grid*):

$$\begin{aligned}
&-\frac{1}{\sqrt{g_{22}}}\frac{g_{12}}{g_{11}}\begin{Bmatrix}2\\1\,2\end{Bmatrix}U^{(1)}U^{(2)}=-\left[\frac{1}{\sqrt{g_{22}}}\frac{\sqrt{g_{11}g_{22}}\cos\theta}{g_{11}}\right]\frac{1}{J}[(x_\xi y_{\xi\eta}-y_\xi x_{\xi\eta})]u_s u_n\\
&=-\left[\frac{\sqrt{g_{11}}\cos\theta}{g_{11}}\right]\frac{1}{\sqrt{g_{11}g_{22}}\sin\theta}\left[\frac{\partial}{\partial\eta}\left(\frac{y_\xi}{x_\xi}\right)x_\xi^2\right]u_s u_n=-\frac{\cos\theta}{\sin\theta}\frac{x_\xi^2}{g_{11}}\frac{\partial}{\sqrt{g_{22}}\partial\eta}\left(\frac{y_\xi}{x_\xi}\right)u_s u_n\\
&=-\frac{\cos\theta}{\sin\theta}\frac{x_\xi^2}{(x_\xi^2+y_\xi^2)}\frac{\partial}{\partial n}\left(\frac{y_\xi}{x_\xi}\right)u_s u_n=-\frac{\cos\theta}{\sin\theta}\frac{1}{[1+(y_\xi/x_\xi)^2]}\frac{\partial}{\partial n}\left(\frac{y_\xi}{x_\xi}\right)u_s u_n\\
&=-\cot\theta\frac{1}{1+k_s^2}\frac{\partial k_s}{\partial n}u_s u_n
\end{aligned} \tag{A20}$$

where k_s denotes the inclination of s line and, $\partial k_s/\partial n$ denotes the variation of s line's inclination along the direction of n line. It can be seen from Equation (A20) that source term (2a) will be equal to 0 if s line is orthogonal to n line.

(6) *Source term* (2b) (*Corioli force caused by the n line's distortion of grid*):
Similar to (5), we may have

$$\frac{1}{\sqrt{g_{11}}}\sqrt{\frac{g_{11}}{g_{22}}}\begin{Bmatrix}1\\2\,1\end{Bmatrix}U^{(2)}U^{(1)}=\frac{1}{\sin\theta}\frac{1}{1+(1/k_n)^2}\frac{\partial}{\partial s}\left(\frac{1}{k_n}\right) \tag{A21}$$

where k_n denotes the inclination of n line, and $\partial/\partial s(1/k_n)$ denotes the variation of $1/k_n$ along the direction of s line.

(7) *Source term* (3a) (*the force caused by the pressure difference in s direction*):

$$\begin{aligned}
\frac{\sqrt{g_{11}}}{\rho}g^{11}\frac{\partial P}{\partial\xi}&=\frac{\sqrt{g_{11}}}{\rho}\frac{g_{22}}{J^2}\frac{\partial P}{\partial\xi}=\frac{1}{\rho}\frac{\sqrt{g_{11}g_{22}}}{g_{11}g_{22}\sin^2\theta}\frac{\partial P}{\partial\xi}=\frac{1}{\sin^2\theta}\frac{1}{\rho}\frac{\partial P}{\sqrt{g_{11}}\partial\xi}\\
&=\frac{1}{\sin^2\theta}\frac{1}{\rho}\frac{\partial P}{\partial s}
\end{aligned} \tag{A22}$$

(8) *Source term* (3b) (*the force caused by the pressure difference in n direction*):

$$-\frac{\sqrt{g_{11}}}{\rho}g^{12}\frac{\partial P}{\partial\eta}=-\frac{\sqrt{g_{11}}}{\rho}\frac{g_{12}}{J^2}\frac{\partial P}{\partial\eta}=-\frac{\sqrt{g_{11}}}{\rho}\frac{\sqrt{g_{11}g_{22}}\cos\theta}{g_{11}g_{22}\sin^2\theta}\frac{\partial P}{\partial\eta}=-\frac{\cos\theta}{\sin^2\theta}\frac{1}{\rho}\frac{\partial P}{\partial n} \tag{A23}$$

(9) *Source term* (4a) (*the friction force acting on river bed in s direction*)

Similar to contra-variant physical velocity component $U^{(1)}$, we may also reduce that $T^{(1)}$ actually are the conventional physical friction stresses τ_s acting on channel bed along s in physical space.

$$\frac{T^{(1)}}{\rho h_s} = \frac{\tau_s}{\rho h_s} \tag{A24}$$

Finally, putting the above terms of (1)–(9) into Equation (A1), we may obtain the transformed equation expressed in a physical form as

$$\begin{aligned} u_s \frac{\partial u_s}{\partial s} + u_n \frac{\partial u_s}{\partial n} + \frac{\cos\theta}{\sin\theta}\frac{u_s^2}{r_s} - \frac{1}{\sin\theta}\frac{u_n^2}{r_n} + \frac{1}{\sin\theta}\frac{u_s u_n}{[1+(1/k_n)^2]}\frac{\partial(1/k_n)}{\partial s} \\ - \frac{\cos\theta}{\sin\theta}\frac{u_s u_n}{1+k_s^2}\frac{\partial k_s}{\partial n} + \frac{1}{\sin^2\theta}\frac{1}{\rho}\frac{\partial P}{\partial s} - \frac{\cos\theta}{\sin^2\theta}\frac{1}{\rho}\frac{\partial P}{\partial n} + \frac{\tau_s}{\rho h_s} = 0 \end{aligned} \tag{A25}$$

In the calculation, the geometric parameters of $\sin\theta, \cos\theta, k_s, k_n$ can be calculated easily by Equations (A26)–(A28) based on the co-ordinate data of mesh (x_i, y_i). That means no matter how complicated the calculation objective's shape is, the calculation of these geometric parameters is very easy and would not be a problem.

$$\sin\theta = \sin(\alpha - \beta) = \sin\alpha \times \cos\beta - \cos\alpha \times \sin\beta \tag{A26}$$

$$\cos\theta = \cos(\alpha - \beta) = \cos\alpha \times \cos\beta + \sin\alpha \times \sin\beta \tag{A27}$$

$$k_s = \frac{y_{i+1,j} - y_{i,j}}{x_{i+1,j} - x_{i,j}}, \qquad k_n = \frac{y_{i,j+1} - y_{i,j}}{x_{i,j+1} - x_{i,j}} \tag{A28}$$

where

$$\sin\alpha = \frac{y_{i,j+1} - y_{i,j}}{\sqrt{(x_{i,j+1} - x_{i,j})^2 + (y_{i,j+1} - y_{i,j})^2}} \tag{A29}$$

$$\cos\alpha = \frac{x_{i,j+1} - x_{i,j}}{\sqrt{(x_{i,j+1} - x_{i,j})^2 + (y_{i,j+1} - y_{i,j})^2}} \tag{A30}$$

$$\sin\beta = \frac{y_{i+1,j} - y_{i,j}}{\sqrt{(x_{i+1,j} - x_{i,j})^2 + (y_{i+1,j} - y_{i,j})^2}} \tag{A31}$$

$$\cos\beta = \frac{x_{i+1,j} - x_{i,j}}{\sqrt{(x_{i+1,j} - x_{i,j})^2 + (y_{i+1,j} - y_{i,j})^2}} \tag{A32}$$

where α denotes the angle between n line and x co-ordinate, and β denotes the angle between s line and x co-ordinate.

REFERENCES

1. Shimizu Y, Itakura T. Calculation of bed variation in alluvial channels. *Journal of Hydrologic Engineering ASCE* 1989; **116**(3):367–384.
2. Liu B-Y, Ashida K, Egshira S. Sediment sorting and its simulation model in meander streams. *Proceedings of the 24th IAHR Congress*, Madrid, Spain, 1991; A453–A460.
3. Fletcher CAJ. Computational techniques for fluid dynamics. *Fundamental and General Techniques* (2nd edn), vol. II. Springer: Berlin, 1991; 47–78.
4. Koshizuka S, Oka Y, Kondo S. A staggered differencing technique on boundary-fitted curvilinear grid for incompressible Navier–Stokes equation written with physical components. *A Collection of Technical Papers*, *3rd International Symposium on Computational Fluid Dynamics*, Nagoya, Japan, 1989.
5. Koshizuka S, Oka Y, Kondo S. A boundary-fitted staggered difference method for incompressible flow using Riemann geometry. *Proceedings of the 1st International Conference on Supercomputing in Nuclear Applications*, Mito, Japan, 1990.
6. Koshizuka S, Oka Y, Kondo S. A staggered differencing technique on boundary-fitted curvilinear grids for incompressible flows along curvilinear or slant walls. *Journal of Computer Mechanics* 1990; **7**:123–136.
7. Demirdzic I, Gosman AD, Issa RI, Peric M. A calculation procedure for turbulent flow in complex geometries. *Computers & Fluids* 1987; **15**:251–273.
8. Takizawa A, Koshizuka S, Kondo S. Generalization of physical component boundary fitted co-ordinate (PCBFC) method for the analysis of free-surface flow. *International Journal for Numerical Methods in Fluids* 1992; **15**:1213–1237.
9. Patankar SV. *Numerical Heat Transfer and Fluid Flow*. Hemisphere: Washington, DC, 1980.

